

Supporting Information

Fig. S1 shows an AFM line scan of a silver line pattern. A structure width of $10\ \mu\text{m}$ and a line height of $80\ \text{nm}$ can be extracted. Furthermore, some nanoparticles between the lines are observed leading to parasitic absorption.

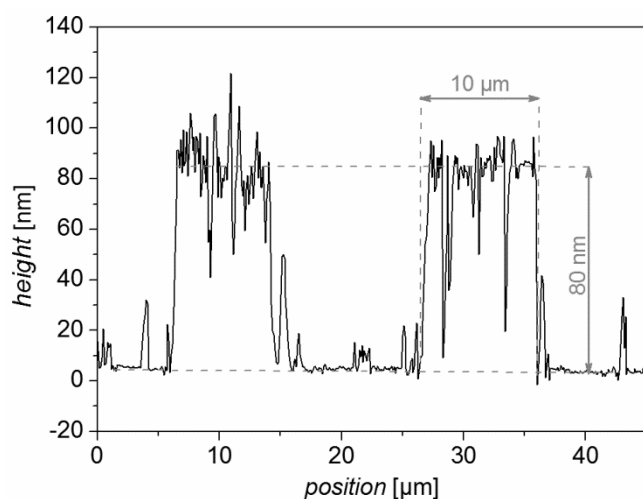


Figure S1: AFM line scan of silver line pattern prepared with a $10\ \mu\text{m}$ line/ $10\ \mu\text{m}$ distance stamp.

Fig. S2 shows an AFM line scan of a silver grid. It can be seen, that $15\ \text{nm}$ lower features compared to line patterns are obtained. In both cases compact and dense silver features have formed, enabling good electrical conductivity.

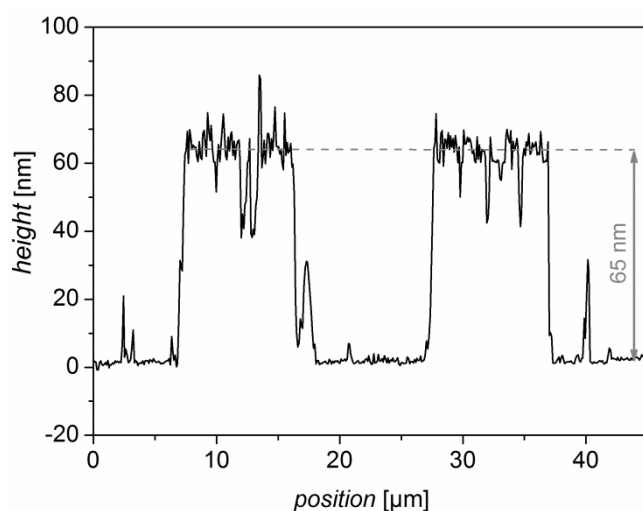


Figure S2: AFM line scan of a silver grid prepared with a $10\ \mu\text{m}$ squared stamp.

Fig. S3 shows XRD patterns of three different samples. The lower curve was taken from the prepared silver citrate (Ag_3Cit). The polymeric precursor was UV photo-reduced (10 minutes in a *Hönle UVACUBE Inert*) resulting in a black precipitate. Powder XRD analysis of this precipitate shows that silver particles are formed. Some crystalline impurities and some inorganic material can be found as well. The upper curve was measured with the residue from the DTA/TG measurement. It is obvious that silver can be pointed out as the only crystalline phase. No impurities or amorphous material is detected.

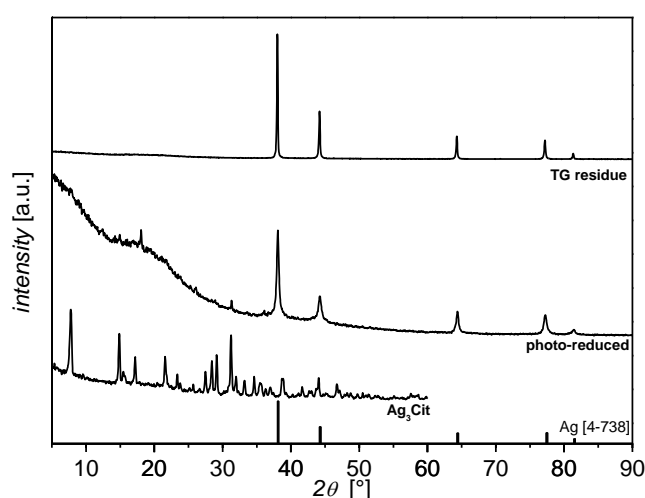


Figure S3: Powder XRD patterns of silver citrate (bottom) UV-reduced polymeric precursor (middle) and TG residue (top). The reference bars indicate silver.

The SEM analysis of the TG residue (Fig. S4) shows a dense material with grain sizes in the range of 100 – 1000 nm. The material offers low porosity as expected from the slow temperature ramp. The round shape of the structures indicate a derivation from a polymeric material conserved due to the careful decomposition.

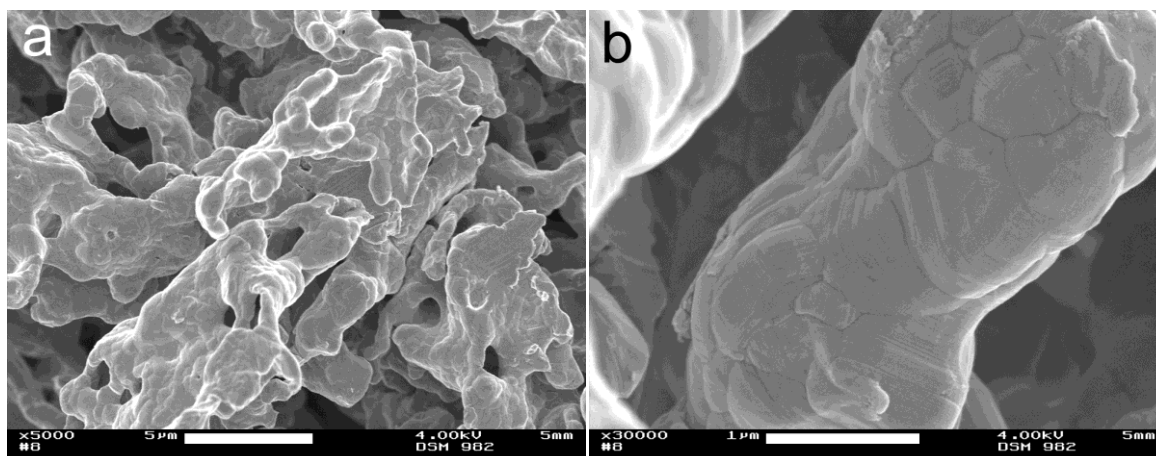


Figure S4: SEM images of the TG residue at a magnification of 5000x (a) and 30000x (b).

The change of the silver films' sheet resistance was measured at different times after reaching 250 °C. Keeping the temperature constant at 250 °C results in a decline from 10.2 Ω to 1.5 Ω after 60 minutes (cf. Fig. S5). This can be attributed to further material decomposition accompanied with better electrical contacts between the silver particles. Longer durations lead again to slightly higher values. Thus, the optimal treatment duration can be pointed out as 60 minutes at 250 °C. After 24 hours the sheet resistance still offers better values than the initial sample. Increasing values above 60 minutes indicate the formation of silver islands and less contact area between these particles.

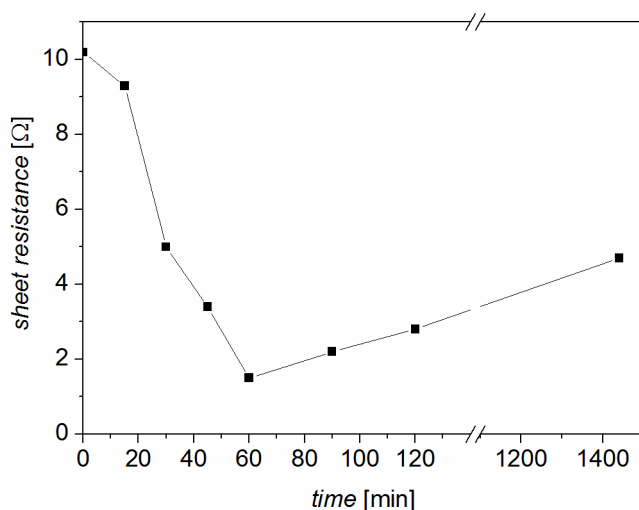


Figure S5: Influence of the treatment duration at 250 °C on the sheet resistance of silver films prepared from polymeric precursor.

To investigate the effects of mechanical bending on the electrical performance of a silver film, we carried out bending tests. A silver coated 25 x 25 cm² PI foil is bent until two opposing edges touch each other. This procedure is repeated 1000 times. Fig. S6 shows the electrical resistivity of the film as a function of bending cycle. An increasing resistivity is observed after 250 bending cycles resulting in an plateau around $4 \cdot 10^{-7} \Omega \text{ m}$. The inset in this diagram shows the film after the bending experiment. A two point measurement shows a resistance of 10.4 Ω across the film.

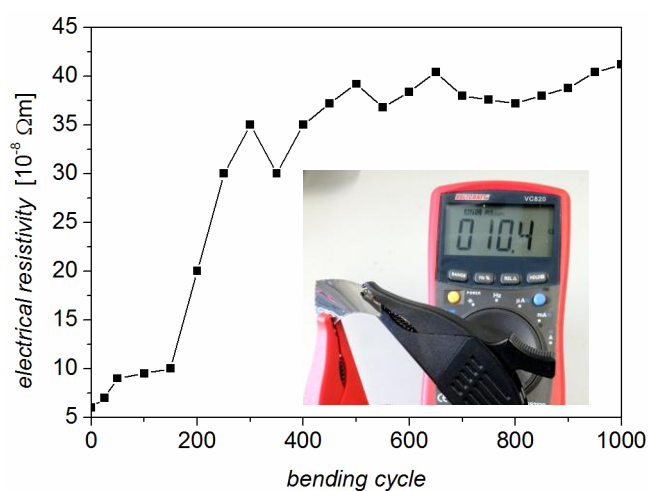


Figure S6: Photograph of a polyimide foil coated with a conductive silver film prepared from polymeric precursor. The inset shows the foil after the bending test in a two point resistance measurement.